

# Magnetic and superconducting properties of $\text{FeSe}_{1-x}\text{Te}_x$ ( $x \simeq 0, 0.5, \text{ and } 1.0$ )

A.V. Fedorchenko<sup>1</sup>, G.E. Grechnev<sup>1</sup>, V.A. Desnenko<sup>1</sup>, A.S. Panfilov<sup>1</sup>, S.L. Gnatchenko<sup>1</sup>,  
V.V. Tsurkan<sup>2,3</sup>, J. Deisenhofer<sup>2</sup>, H.-A. Krug von Nidda<sup>2</sup>, A. Loidl<sup>2</sup>, D.A. Chareev<sup>4</sup>,  
O.S. Volkova<sup>5</sup>, and A.N. Vasiliev<sup>5</sup>

<sup>1</sup> *B. Verkin Institute for Low Temperature Physics and Engineering of the National Academy of Sciences of Ukraine  
47 Lenin Ave., Kharkov 61103, Ukraine  
E-mail: panfilov@ilt.kharkov.ua*

<sup>2</sup> *Experimental Physics 5, Center for Electronic Correlations and Magnetism, Institute of Physics  
University of Augsburg, Augsburg 86159, Germany*

<sup>3</sup> *Institute of Applied Physics, Academy of Sciences of Moldova, MD-2028 Chisinau, Republic of Moldova*

<sup>4</sup> *Institute of Experimental Mineralogy, Russian Academy of Sciences  
Chernogolovka, Moscow District 142432, Russia*

<sup>5</sup> *Moscow State University, Physics Department, Moscow 119991, Russia*

Received October 12, 2010

Magnetization studies for  $\text{FeSe}_{1-x}\text{Te}_x$  ( $x \simeq 0, 0.5, \text{ and } 1.0$ ) compounds were carried out in magnetic fields up to 50 kOe and in the temperature range 2–300 K. The superconducting transition was observed at  $T_c \simeq 8$  K and 13.6–14.2 K in  $\text{FeSe}_{0.963}$  and  $\text{FeSe}_{0.5}\text{Te}_{0.5}$ , respectively. For the most samples, a nonlinear behavior of the magnetization curves in the normal state gives evidence of a commonly observed substantial presence of ferromagnetic impurities in the compounds under study. By taking these impurity effects into account, the intrinsic magnetic susceptibility  $\chi$  of  $\text{FeSe}_{0.963}$ ,  $\text{FeSe}_{0.5}\text{Te}_{0.5}$ , and  $\text{FeTe}$  was estimated to increase gradually with Te content. For  $\text{FeTe}$  a drastic drop in  $\chi(T)$  with decreasing temperature was found at  $T_N \simeq 70$  K, which is presumably related to antiferromagnetic ordering. To shed light on the observed magnetic properties, *ab initio* calculations of the exchange enhanced magnetic susceptibility are performed for  $\text{FeSe}$  and  $\text{FeTe}$  within the local spin density approximation.

PACS: 74.70.Xa Pnictides and chalcogenides;  
74.20.Pq Electronic structure calculations;  
74.25.Ha Magnetic properties;  
75.30.Cr Saturation moments and magnetic susceptibilities.

Keywords:  $\text{FeSe}$ ,  $\text{FeTe}$ , high-temperature superconductivity, magnetization, electronic structure.

## 1. Introduction

Following recent discovery of the iron-pnictide high  $T_c$  superconductors (SCs) [1,2], a search for the new SCs rapidly extended to a large variety of iron-based planar compounds [3–8]. Among them, iron chalcogenides  $\text{FeSe}_{1-x}\text{Te}_x$  are distinguished by their structural simplicity [9]. They belong to so-called «11»-type iron-based SCs and consist of the iron-chalcogenide layers with square planar sheets of Fe in a tetrahedral Se (or Te) environment, maintaining

the same  $\text{Fe}^{+2}$  charge state as the iron pnictides. The SC with modest transition temperature about  $T_c \simeq 8$  K was observed for Se deficient  $\text{FeSe}$  compounds [9–11], whereas partial replacing of Se with Te has provided  $T_c \simeq 15$  K at about 50% Te substitution [12,13]. However, the recent reports on SC of  $\text{FeSe}$  under high pressures with  $T_c \simeq 27$  K [14], 34 K [15], 35 K [16], and 37 K [17,18] have stimulated considerable interest to physical properties of  $\text{FeSe}_{1-x}\text{Te}_x$ .

The electron-phonon interaction is estimated to be too small in the iron-based SCs to provide the conventional superconductivity, and there is growing anticipation that superconductivity in the iron-based SCs is driven by spin-fluctuations due to proximity to magnetic instability in FeSe and related compounds [7,19,20]. The itinerant spin-density-wave (SDW) transitions were established in parent compounds of the Fe based SCs, which are resulted in relatively small ordered magnetic moments, and in essentially non-Curie-Weiss behavior of magnetic susceptibility with temperature above  $T_{SDW}$  [3–6]. On the other hand, the undoped FeTe compound is not superconducting but magnetically ordered [13,21,22]. Moreover, the magnetic structure found in the FeTe compound is rather different from that of parent iron-arsenide SC compounds, despite the same Fermi surface nesting predicted by DFT calculations [7,19]. It was suggested that the electrons in  $\text{FeTe}_{1-x}\text{Se}_x$  system are localized and close to Mott–Hubbard transition, with the local magnetic moments interacting via short-range superexchange [23], and the superconductivity is promoted by a combination of resonant valence bond and excitonic insulator physics [8].

At the present time, there is considerable controversy regarding an interplay between electronic structure, magnetism and superconductivity in  $\text{FeSe}_{1-x}\text{Te}_x$  compounds, and their complex magnetic properties are still not well characterized and understood. The experimental data on magnetic susceptibility behavior of  $\text{FeSe}_{1-x}\text{Te}_x$  systems in the normal state are still incomplete and contradicting [12,13,21]. Also, the magnetic behaviors of  $\text{FeSe}_{1-x}\text{Te}_x$  systems are presumably related to the presence of magnetic impurities and secondary phases. Therefore, further studies of magnetic and superconducting properties and their evolution with doping, pressure, and temperature can help to elucidate a mechanism of the high- $T_c$  superconductivity in this family of the Fe-based SCs.

In order to elucidate the superconducting mechanism and its relation with the expected effect of spin fluctuations, it is very important to obtain the intrinsic susceptibility of the Fe-based SCs. In this contribution we report the experimental results on magnetic susceptibility studies for the  $\text{FeSe}_{1-x}\text{Te}_x$  compounds in the normal state. The main objective of this study is to reveal and separate magnetic properties of the parent phase from contributions of secondary phases and impurities. The experimental study is supplemented by *ab initio* calculations of the electronic structure and magnetic susceptibility of FeSe and FeTe within the density functional theory (DFT). Therefore, the aim of this investigation is to shed more light on the relation between magnetic properties and the chemical and structural composition, and also on the interplay between superconductivity and magnetic instability in the  $\text{FeSe}_{1-x}\text{Te}_x$  system.

## 2. Experimental details and results

The polycrystalline  $\text{FeSe}_{0.963}$  and  $\text{FeTe}_{0.95}$  samples were obtained by conventional solid-state synthesis. The starting chemicals were powder iron (Merck, 99.5%, 10  $\mu\text{m}$ ) and crystalline selenium and tellurium cleaned by the floating zone method. These chemicals were mixed in proportions consistent with the stoichiometry of reaction,  $\text{Fe}:\text{Se} = 1:0.963$  and  $\text{Fe}:\text{Te} = 1:0.95$ , sealed in an evacuated ( $10^{-4}$  bar) silica glass capsule, and annealed at 700 K for 14 days. The reacted mixture was ground in an agate mortar under acetone and then pressed into pellets of 6 mm in diameter at the load of 1–1.2 tons, followed by annealing in the evacuated silica glass capsule at 700 K for 20 days. Both synthesized substances were examined under a microscope in reflected light and analyzed by x-ray powder diffraction (XRD,  $\text{Co K}_\alpha$  radiation, Fe filter) and by electron microanalysis (CAMECA SX100, 15 kV).

The single crystals with  $x \simeq 0.5$  and 1 were grown by a slow cooling with the self-flux method [24], and two series of samples have been prepared. The phase content of the samples was checked by x-ray diffraction. Hereafter, we will refer to the polycrystalline and single-crystalline samples as P and S, respectively, followed by the series number. The dc magnetization studies were carried out in the magnetic field up to 50 kOe and the temperature range 2–300 K using a superconducting quantum interference device (SQUID) magnetometer. For single crystals the magnetic field was applied along the tetragonal  $c$ -axis.

The temperature dependences of the magnetic susceptibility  $\chi(T)$  measured in the low magnetic field (see Fig. 1) exhibit few clear peculiarities. The low temperature peculiarities are related to the superconducting transitions at  $T_c \sim 8$  and 13.5 K for  $\text{FeSe}_{0.963}$  (P) and  $\text{FeSe}_{0.5}\text{Te}_{0.5}$  (S1), respectively. The detailed data on SC transition for the  $\text{FeSe}_{0.5}\text{Te}_{0.5}$  single crystals are shown in Fig. 2. The value  $T_c \simeq 14.2$  K resulted for the sample of the second series is close to the maximum  $T_c$  value observed at ambient pressures in the  $\text{FeSe}_{1-x}\text{Te}_x$  family for  $x \sim 0.5$  [12,25].

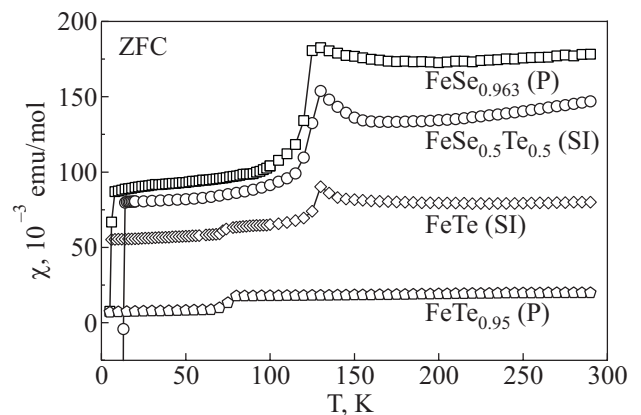


Fig. 1. Temperature dependence of the magnetic susceptibility for  $\text{FeSe}_{0.963}$ ,  $\text{FeSe}_{0.5}\text{Te}_{0.5}$ , and FeTe ( $\text{FeTe}_{0.95}$ ) measured in the magnetic field  $H = 200$  Oe and zero field cooling (ZFC).

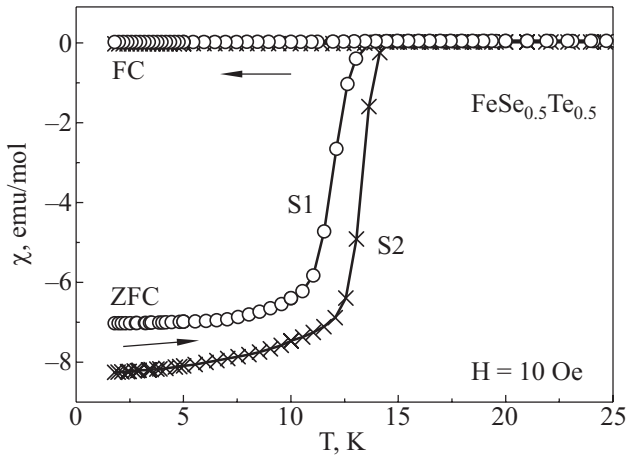


Fig. 2. Low field magnetic susceptibility in vicinity of the superconducting transition for FeSe<sub>0.5</sub>Te<sub>0.5</sub> single crystals of two series S1 and S2.

Also, the pronounced anomalies of  $\chi(T)$  are seen in Fig. 1 at 125 K. Below this temperature  $\chi(T)$  exhibits a remarkable irreversibility between zero-field cooling (ZFC) and field cooling (FC, not shown in the figure) magnetization data. Such behavior may be due to the magnetite (Fe<sub>3</sub>O<sub>4</sub>) impurities and related to the Verwey transition, which is observed in magnetite at  $T_V \sim 120\text{--}125$  K (see [26] and references therein).

In addition, a threshold cusp in  $\chi(T)$  appears near 70 K for FeTe (S1) and FeTe<sub>0.95</sub> (P). According to the recent neutron-scattering measurements for FeTe [21,22] this peculiarity corresponds to an antiferromagnetic (AFM)

ordering with a rather complex magnetic structure and the simultaneous structural transition from a tetragonal lattice (at high temperatures) to a distorted orthorhombic phase.

A relatively large content of ferromagnetic (FM) impurities in the studied samples is readily illustrated by the magnetization data  $M(H)$  in Fig. 3. Generally, at high magnetic fields the  $M(H)$  dependencies show a linear behavior (dashed lines in Fig. 3) with a slope determined by the host (i.e. intrinsic) magnetic susceptibility of the sample. By their extrapolation to the zero field we obtained the saturation moment values of FM impurities for our samples, which fall in the range from 25 to 300 emu/mol, being weakly dependent on temperature.

Despite the pronounced FM impurity effects, the obtained magnetization data in Fig. 3 make it possible to estimate with sufficient accuracy the host magnetic susceptibilities  $\chi_{\text{host}}$  for our samples from the slope of linear part of corresponding  $M(H)$  dependence at high fields. The resulted values of  $\chi_{\text{host}}$  at some fixed temperatures are shown by full circles in Fig. 4. In Fig. 4 we also presented the detailed  $\chi_{\text{host}}(T)$  data, which were obtained according to the equation,

$$\chi(T) \equiv \chi_{\text{host}}(T) = (M(T) - M_s) / H, \quad (1)$$

from temperature dependence of the magnetization  $M(T)$  measured in magnetic field of 30 kOe. Here the saturation moment value  $M_s$  of FM impurity is assumed to be constant and equal to its temperature-averaged value for a given sample.

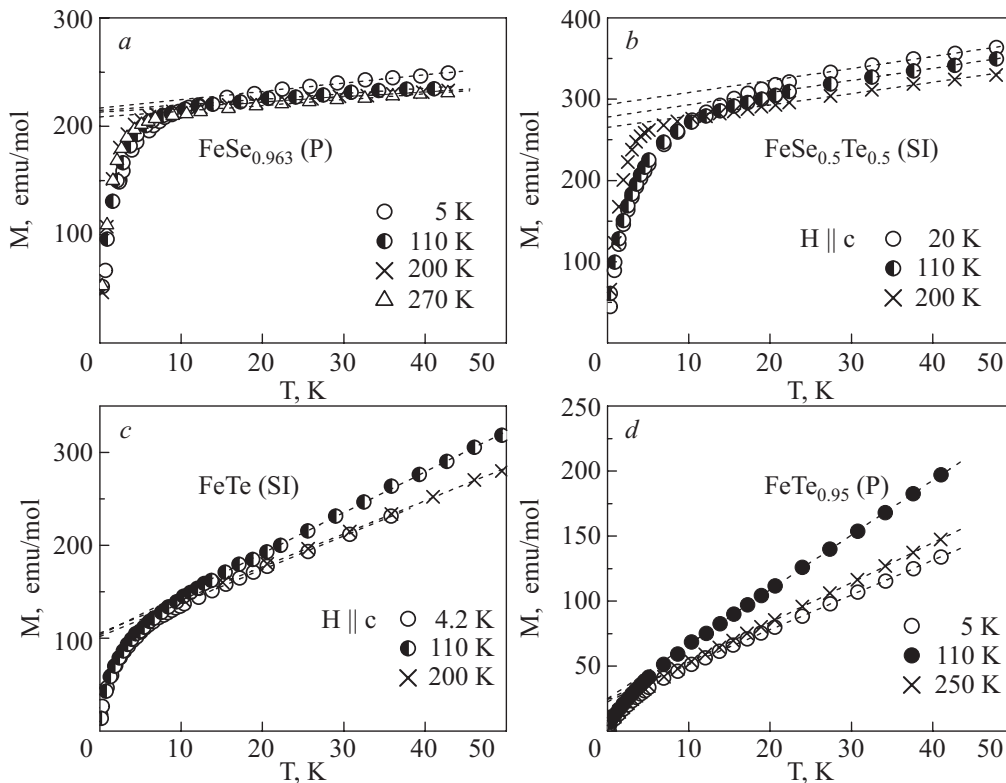


Fig. 3. Magnetization data for some FeSe<sub>1-x</sub>Te<sub>x</sub> compounds at different temperatures.

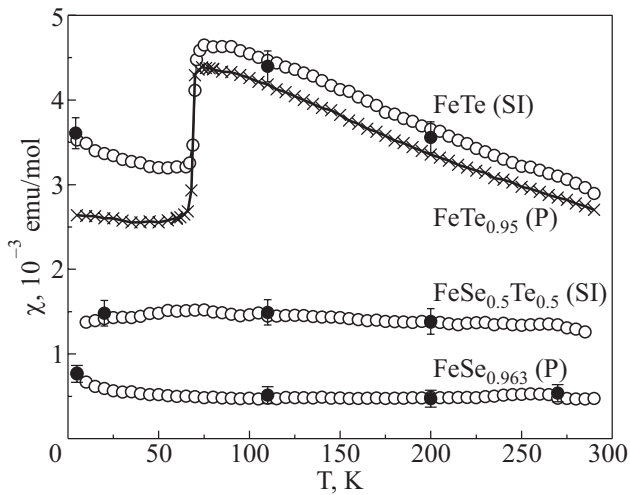


Fig. 4. Temperature dependence of the host magnetic susceptibility for some  $\text{FeSe}_{1-x}\text{Te}_x$  compounds. Full circles correspond to values derived from the high field magnetization data in Fig. 3.

In Fig. 5 the magnetization data are shown for some selected temperatures for  $\text{FeSe}_{0.5}\text{Te}_{0.5}$  and  $\text{FeTe}$  single

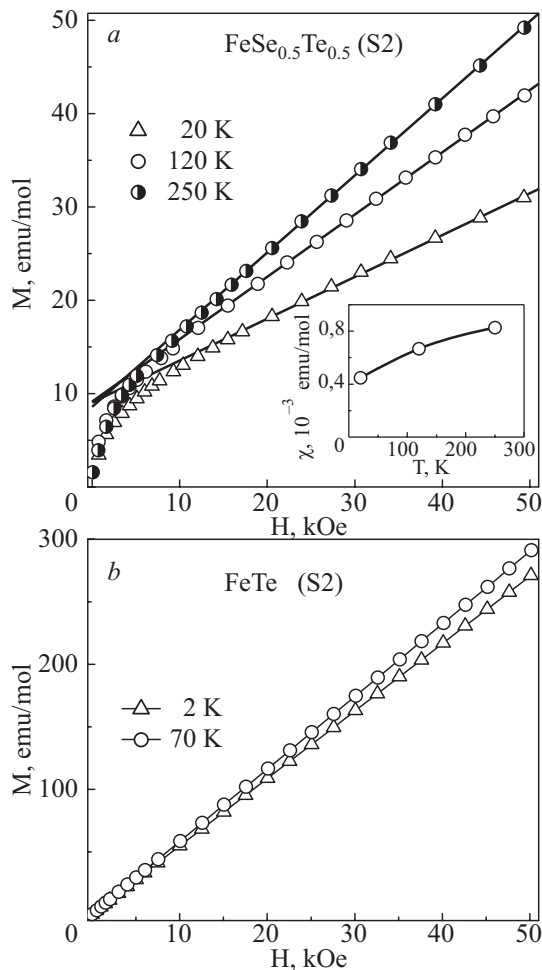


Fig. 5. Magnetization data for  $\text{FeSe}_{0.5}\text{Te}_{0.5}$  (a) and  $\text{FeTe}$  (b) single crystals of the second series (S2) at different temperatures. In inset are the values of the host magnetic susceptibility versus temperature for  $\text{FeSe}_{0.5}\text{Te}_{0.5}$ , derived from its high field magnetization data.

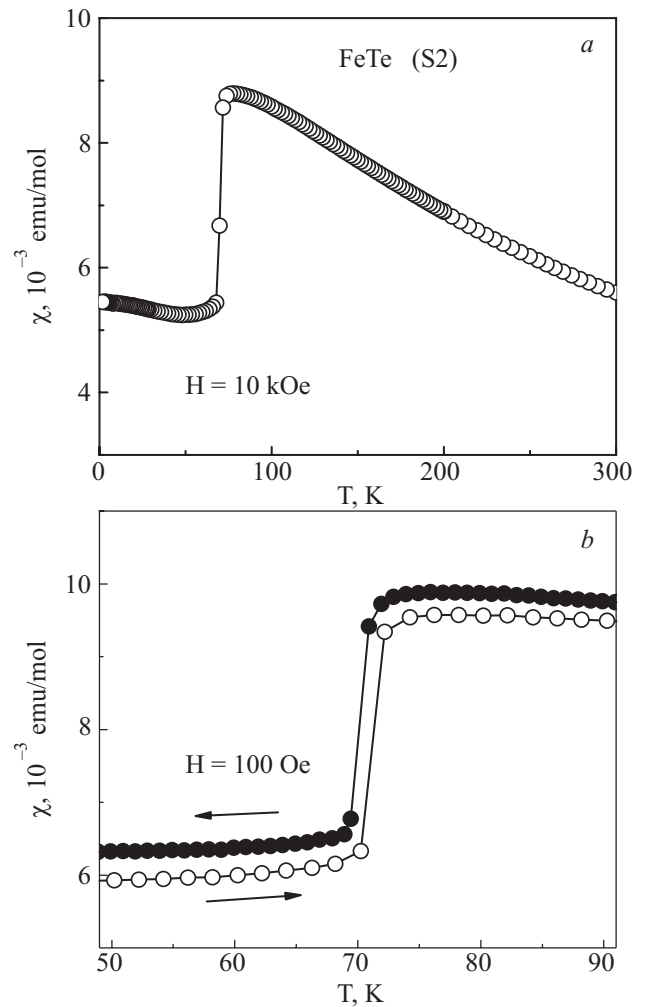


Fig. 6. Temperature dependence of the magnetic susceptibility for  $\text{FeTe}$  (S2) single crystal (a) and its hysteresis behavior (b) in vicinity of the phase transition at  $T \simeq 70$  K.

crystals of the second series. Compared to the first series (see Fig. 3,b), the  $\text{FeSe}_{0.5}\text{Te}_{0.5}$  sample appeared to have much smaller saturation moment of FM impurities. In addition, the temperature dependence of its host magnetic susceptibility (inset in Fig. 5,a) is distinctly different from that of the first series sample (Fig. 4) both in character and in magnitude of the susceptibility values. As is evident from a linear  $M(H)$  dependence for  $\text{FeTe}$  in Fig. 5,b, there are no any detectable FM impurities in this sample. The temperature dependence of its magnetic susceptibility given in Fig. 6,a exhibits almost the same behavior in vicinity of the phase transition as  $\chi(T)$  of the polycrystalline  $\text{FeTe}_{0.95}$  sample and  $\text{FeTe}$  single crystal of the first series (see Fig. 4) but has more pronounced magnitude of the effect. A small hysteresis in  $\chi(T)$  dependence is observed after heating the sample to about 200 K and subsequent cooling below the transition temperature (Fig. 6,b). A similar  $\chi(T)$  behavior for  $\text{FeTe}$  was also reported in Ref. 22.

The experimentally obtained basic superconducting and magnetic characteristics of the studied samples are summarized in Table 1.

Table 1. Superconducting transition temperature  $T_c$  (in K), FM impurity saturation magnetic moment  $M_s$  (emu/mol) and host (intrinsic) magnetic susceptibility  $\chi$  ( $10^{-3}$  emu/mol) at room and zero temperatures for  $\text{FeTe}_{1-x}\text{Se}_x$  compounds.

Compound	$T_c$	$M_s$	$\chi$	
			290 K	0 K
$\text{FeSe}_{0.963}$ (P)	$\sim 7$	214	$0.5 \pm 0.1$	$0.75 \pm 0.1$
$\text{FeSe}_{0.5}\text{Te}_{0.5}$ (S1)	13.5	280	$1.3 \pm 0.2$	$1.45 \pm 0.2$
$\text{FeSe}_{0.5}\text{Te}_{0.5}$ (S2)	14.2	9	$0.85 \pm 0.1$	$0.4 \pm 0.1$
$\text{FeTe}_{0.95}$ (P)	–	24	$2.7 \pm 0.2$	$2.65 \pm 0.2$
$\text{FeTe}$ (S1)	–	103	$2.9 \pm 0.2$	$3.6 \pm 0.2$
$\text{FeTe}$ (S2)	–	$\sim 0$	$5.7 \pm 0.2$	$5.45 \pm 0.2$

### 3. Computational details and results

To gain a further insight into magnetic properties of the  $\text{FeSe}_{1-x}\text{Te}_x$  system in the normal state, the *ab initio* calculations of the electronic structure and exchange enhanced magnetic susceptibility are performed for FeSe and FeTe parent compounds within DFT and the local spin density approximation.

At ambient conditions the  $\text{FeSe}_{1-x}\text{Te}_x$  compounds possess the tetragonal PbO-type crystal structure (space group  $P4/nmm$ ), which exhibits strong two-dimensional features. The crystal lattice is composed by alternating triple-layer slabs, which are stacked along the  $c$ -axis. Each iron layer is sandwiched between two nearest-neighbor chalcogen layers, which form edge-shared tetrahedrons around the iron sites. The positions of Se (or Te) sheets are fixed by the internal parameter  $Z$ , which represents the height of chalcogen atoms above the iron square plane. This parameter also determines the chalcogen-Fe bond angles. Crystal structure parameters of  $\text{FeSe}_{1-x}\text{Te}_x$  compounds were established in a number of works by means of x-ray and neutron diffraction studies [11,13,14,21,22].

The previous *ab initio* calculations of the electronic structure of the «11»-type iron-based chalcogenides were predominantly related to studies of the AFM and SDW ordering [19,20,23,31–34]. In this paper the electronic structure calculations are carried out for FeSe and FeTe compounds with the aim to study a paramagnetic response in an external magnetic field, and to elucidate a nature of paramagnetism and magnetic instability in the parent phases of «11» systems. The *ab initio* calculations are carried out by employing a full-potential all-electron relativistic linear muffin-tin orbital method (FP-LMTO, code RSPt [35,36]). No shape approximations were imposed on the charge density or potential, what is especially important for the anisotropic layered crystal structures. The exchange-correlation potential was treated within the local spin density approximation (LSDA, [37]) of the density functional theory. The calculations were based on the experimental lattice parameters from Refs. 10, 11, 13, 14, 21, 22.

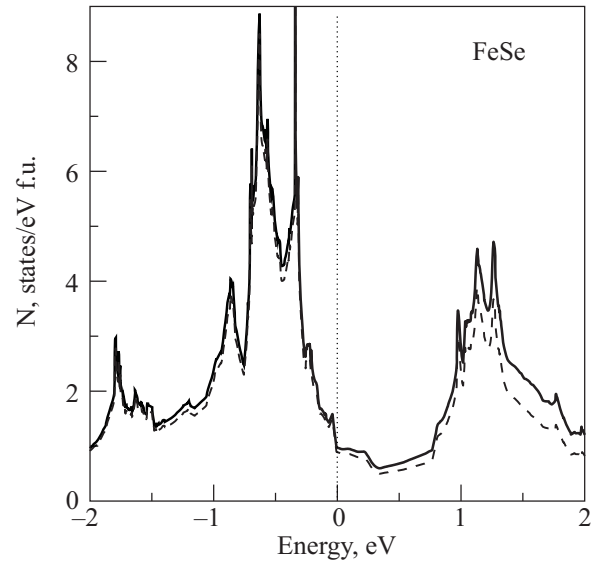


Fig. 7. Total density of states of the paramagnetic FeSe around  $E_F$  (solid line) and the partial contribution of the iron  $d$ -states (dashed line). The Fermi level position (at 0 eV) is marked by a vertical line.

The calculated basic features of electronic structure of FeSe and FeTe are in a qualitative agreement with results of earlier calculations [19]. In particular, the detailed density of states (DOS)  $N(E)$  of FeSe is presented in Fig. 7. In the vicinity of the Fermi level  $E_F$  the  $d$ -states of Fe provide the dominant contribution to DOS in the range  $-2$  eV and 2 eV around  $E_F = 0$ . The  $p$  states of chalcogen atoms are predominantly extended in the interstitial region, and their partial contributions to DOS in vicinity of  $E_F$  are substantially smaller for both FeSe and FeTe. As seen in Fig. 7, in FeSe the Fermi level lies at the steep slope of  $N(E)$ , in the beginning of a pseudogap of about  $\simeq 0.7$  eV. In fact, there is a van Hove singularity in  $N(E)$  at about 0.05 eV below  $E_F$  (see Fig. 6). The calculated  $N(E_F)$  for FeSe can be related to the measured electronic specific heat coefficient,  $\gamma = 9.17$  mJ/mol K<sup>2</sup> [9], by means of the Sommerfeld coefficient formula,  $\gamma = 2\pi^2 k_B^2 N(E_F)(1+\lambda)/3$ . This provides the estimation for the enhancement factor in FeSe:  $\lambda = 3.8$ . Also, the evaluated for FeSe and FeTe volume derivatives  $d \ln N(E_F) / d \ln V$  are found to be positive and equal to 1.25 and 1.42, respectively, what suggests the reduction of  $N(E_F)$  with pressure.

The FP-LMTO-LSDA calculations of the field-induced spin and orbital (Van Vleck) magnetic moments were carried out for FeSe and FeTe self-consistently within the procedure described in Ref. 36 by means of the Zeeman operator,

$$\mathcal{H}_Z = \mu_B \mathbf{H}(2\hat{s} + \hat{\mathbf{l}}), \quad (2)$$

which was incorporated in the original FP-LMTO Hamiltonian. Here  $\mathbf{H}$  is the external magnetic field,  $\hat{s}$  and  $\hat{\mathbf{l}}$  the

spin and orbital angular momentum operators, respectively. The field induced spin and orbital magnetic moments were calculated in the external field of 10 T and provided estimation of the related contributions to the magnetic susceptibility,  $\chi_{\text{spin}}$  and  $\chi_{\text{orb}}$ .

For the tetragonal crystal structure of FeSe, the paramagnetic contributions  $\chi_{\text{spin}}$  and  $\chi_{\text{orb}}$  were derived from the magnetic moments obtained in an external field, applied both parallel and perpendicular to the  $c$  axis. The evaluated magnetic anisotropy, which is determined by the orbital contribution, appeared to be negligible, in comparison with the dominant  $\chi_{\text{spin}}$  contribution. The orbital Van Vleck contribution itself is substantially smaller than the strongly enhanced spin susceptibility, and comes from the  $d$ -states of Fe.

In the course of calculations, we found that magnetic response to the external field is very sensitive to the height  $Z$  of chalcogen species from the Fe plane. The corresponding calculated dependences of magnetic susceptibility for FeSe and FeTe are given in Figs. 8 and 9, respectively. It should be noted here that the itinerant nature of the hybridized  $3d$ -states of Fe is an essential condition for the described above field-induced calculations of paramagnetic susceptibility. There is a strong experimental support for this itinerant picture for FeSe, which is expected to be in a non-magnetic spin-degenerate state. For FeTe, however, a validity of the field-induced calculations of  $\chi$  is questionable due to the expected more localized nature of the  $3d$ -states. For this reason, the calculations for FeTe are performed only for volumes smaller than the experimental volume, and results of these calculations have to be thoroughly verified by other methods, and compared with experimental data.

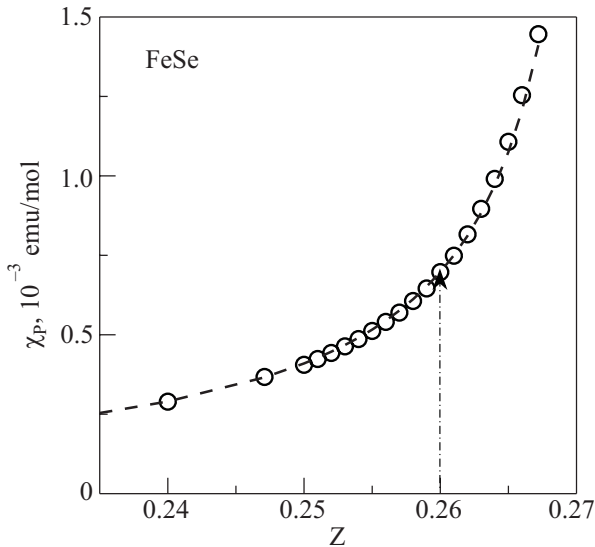


Fig. 8. Calculated paramagnetic susceptibility of FeSe as a function of the internal lattice parameter  $Z$ . The unit cell volume and  $c/a$  ratio are fixed to their experimental ambient pressure values ( $78.4 \text{ \AA}^3$  and  $1.464$  [14]). The dashed line is a guide for the eye. The dashed-dotted line corresponds to the experimental  $Z$ .

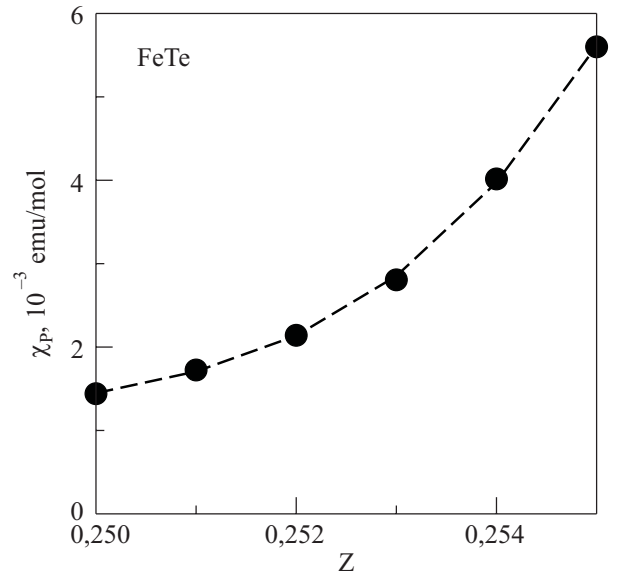


Fig. 9. Calculated paramagnetic susceptibility of FeTe as a function of the internal lattice parameter  $Z$  for LSDA optimized ( $87 \text{ \AA}^3$ ) unit cell volume. The  $c/a$  ratio is fixed to the experimental ambient pressure value ( $1.647$  [14]). The dashed line is a guide for the eye.

The enhanced Pauli spin contribution to the magnetic susceptibility was also calculated within the Stoner model:

$$\chi_{\text{ston}} = S\chi_P \equiv \mu_B^2 N(E_F) [1 - IN(E_F)]^{-1}, \quad (3)$$

where  $\chi_P = \mu_B^2 N(E_F)$ ,  $S$  is the Stoner enhancement factor, and  $\mu_B$  the Bohr magneton. The multi-band Stoner integral  $I$ , representing the exchange-correlation interactions for conduction electrons and appropriate for compounds, can be expressed in terms of the calculated parameters of the electronic structure [38]:

$$I = 1/N(E_F)^2 \sum_{ql'l'} N_{ql}(E_F) J_{ql'l'} N_{ql'}(E_F). \quad (4)$$

Here  $N(E_F)$  and  $N_{ql}(E_F)$  are the total density of electronic states and site,  $q$ , and angular momentum,  $l$ , projected DOS at the Fermi level. The parameters of the exchange interaction  $J_{ql'l'}$  are defined in terms of the intra-atomic exchange integrals:

$$J_{ql'l'} = \int g(\rho(r)) \phi_{ql}(r)^2 \phi_{ql'}(r)^2 dr, \quad (5)$$

and therefore depend upon the corresponding partial wave functions  $\phi_l(r)$ . Here  $g(\rho(r))$  is a function of the electron density [37],  $l$  and  $l'$  are the corresponding angular-momentum quantum numbers.

In the framework of an itinerant model of magnetism the mean field treatment within the Stoner model can be valid at least to establish trends. This model predicts the FeTe system to be unstable in a non-magnetic state. For FeSe the calculated value of the enhanced Pauli susceptibility ( $\chi_{\text{ston}} \sim 0.4 \cdot 10^{-3} \text{ emu/mol}$ ) is close to the field-

induced evaluated  $\chi_{\text{spin}}$  for the same range of lattice parameters. The calculated susceptibility enhancement factor  $S$  appears to be about 10, and this means nearness to a quantum critical point in the pure FeSe compound and a possibility of competition between FM and AFM spin fluctuations.

#### 4. Discussion

The experimental superconducting and magnetic characteristics obtained for the studied  $\text{FeSe}_{1-x}\text{Te}_x$  compounds agree reasonably with those reported in Refs. 13, 22, 27–30. In particular, the intrinsic magnetic susceptibility derived in our work for the normal state of  $\text{FeSe}_{0.963}$  is close to that cited recently in Ref. 27 for polycrystalline  $\text{Fe}_{1.11}\text{Se}$ . The inherent feature of the FeSe–FeTe system resulted from our study is a high sensitivity of the magnetic properties to quality and composition of the samples. This can be readily demonstrated here by the data for  $\text{FeSe}_{0.5}\text{Te}_{0.5}$  and FeTe compounds in Table 1. However, despite an appreciable uncertainty, the obtained experimental data suggest a gradual increase of the magnetic susceptibility in  $\text{FeSe}_{1-x}\text{Te}_x$  system with increasing of tellurium content.

On comparing the experimental  $\chi$  from Table 1 with the calculated ones from Fig. 8 we should note that the experimental internal lattice parameter  $Z$  in FeSe is about 0.26 [10,11,14], whereas the optimized DFT calculated values of  $Z$  are 0.234 [19] and 0.26 [33]. Though the calculated paramagnetic susceptibility is very sensitive to the height  $Z$  of Se atoms from the Fe plane, we can estimate the corresponding contributions to  $\chi$  as  $\chi_{\text{spin}} = 0.55 \cdot 10^{-3}$  emu/mol and  $\chi_{\text{orb}} = 0.11 \cdot 10^{-3}$  emu/mol for the experimental lattice parameters of FeSe ( $V = 78.4 \text{ \AA}^3$ ,  $c/a = 1.464$ ,  $Z = 0.26$  [14]). Therefore the calculated field-induced magnetic moments are in a qualitative agreement with the obtained experimental susceptibility of FeSe in the paramagnetic region (Table 1). Actually, the FeSe compound is found to be on the verge of magnetic instability. The proximity to a quantum critical point is clearly seen in Fig. 8, and this nearness can result in strong spin fluctuations.

For FeTe the Stoner criterion is fulfilled for experimental values of cell volume and parameter  $Z$ . Actually, our self-consistent field-induced LSDA calculations for FeTe converged to the paramagnetic state only for reduced lattice parameters. This is especially relevant to the parameter  $Z$ , which had to be also reduced for about 10%. Therefore we should consider the calculated paramagnetic susceptibility of FeTe in Fig. 9 as a rough estimation which can be valid at least to establish a trend for the effect of  $Z$  parameter. To further address the question to what extent a qualitative agreement between the calculated  $\chi$  and experimental data for FeTe in Table 1 might be fortuitous, the detailed study of pressure effect on  $\chi$  is highly desirable.

A detailed investigation of  $\chi(T)$  and  $\chi(x)$  in  $\text{FeSe}_{1-x}\text{Te}_x$  compounds merits a separate examination beyond the scope of this study. In order to elucidate in a systematic way the effects of isovalent partial substitution of Te for Se in the system, one has to examine an extended concentration range. Also, a further development in technology of samples preparing is desirable. On the theoretical side, a more rigorous calculations technique for FeTe and the alloys is needed, presumably by employing the so-called disordered local moments (DLM) approach [34,39], which seems relevant for the localized states of Fe.

#### 5. Conclusions

Magnetic susceptibility of  $\text{FeSe}_{1-x}\text{Te}_x$  ( $x \simeq 0, 0.5$ , and 1.0) compounds was investigated in the temperature range 2–300 K. The superconducting transitions are detected at 8 K and 13.6–14.2 K in  $\text{FeSe}_{0.963}$  and  $\text{FeSe}_{0.5}\text{Te}_{0.5}$  samples, respectively. For the most samples, a nonlinear behavior of the magnetization curves in the normal state gives evidence of substantial presence of ferromagnetic impurities. By taking these impurity effects into account, the intrinsic magnetic susceptibility  $\chi$  in the series of iron chalcogenides  $\text{FeSe}_{0.963}$ ,  $\text{FeSe}_{0.5}\text{Te}_{0.5}$  and FeTe was estimated to increase gradually with Te content in about ten times.

*Ab initio* calculations of the electronic structure and paramagnetic contributions to susceptibility of the FeSe compound have revealed that this system is in close proximity to the quantum critical point, and this nearness can result in strong spin fluctuations. It is shown, that the paramagnetic susceptibility calculated in external magnetic field appears to be close to the obtained experimental value. The Van Vleck contribution to  $\chi$  in FeSe, which amounts up to 20% of total susceptibility, comes mainly from  $d$ -electrons of Fe, and should not be neglected in comparisons with the experimental data. In general, the numerical results point out that itinerant magnetism theory is relevant to describe magnetic properties of FeSe system.

For FeTe a drastic drop in  $\chi(T)$  with decreasing temperature was found at  $T_N \simeq 70$  K, which is presumably related to antiferromagnetic ordering. The LSDA calculated paramagnetic susceptibility (Fig. 9), being of the same order with the experimental data, reveals a drastic sensitivity to the structural parameter  $Z$ . Therefore, the detailed study of pressure effect on  $\chi$  would be very useful to further address the question about a nature of paramagnetic state in FeTe. Also rigorous calculations of  $\chi$  are required for FeTe, which would take into account disordered local magnetic moments above  $T_N$ . In particular, the recently *ab initio* employed DLM approach [34,39] seems very promising to shed light on behavior of  $\chi(T, P)$ .

The authors dedicate this work to the 100th anniversary of David Shoenberg, who was a pioneer of low-

temperature physics and studies of electronic structure of solids.

This work has been supported by the Russian-Ukrainian RFBR-NASU project 43-02-10 and 10-02-90409.

1. H. Takahashi, K. Igawa, K. Arii, Y. Kamihara, M. Hirano, and H. Hosono, *Nature* **453**, 376 (2008).
2. Z.-A. Ren, W. Lu, J. Yang, W. Yi, X.-L. Shen, Z.-C. Li, G.-C. Che, X.-L. Dong, L.-L. Sun, F. Zhou, and Z.-X. Zhao, *Chin. Phys. Lett.* **25**, 2215 (2008).
3. Yu.A. Izyumov and E.Z. Kurmaev, *Physics Uspekhi* **51**, 1261 (2008).
4. A.L. Ivanovskii, *Physics Uspekhi* **51**, 1201 (2008).
5. M.V. Sadvskii, *Physics Uspekhi* **51**, 1229 (2008).
6. K. Ishida, Y. Nakai, and H. Hosono, *J. Phys. Soc. Jpn.* **78**, 062001 (2009).
7. D.J. Singh, *Physica C* **469**, 418 (2009).
8. J.A. Wilson, *J. Phys.: Condens. Matter* **22**, 203201 (2010).
9. F.C. Hsu, J.Y. Luo, K.W. Yeh, T.K. Chen, T.W. Huang, P.M. Wu, Y.C. Lee, Y.L. Huang, Y.Y. Chu, D.C. Yan, and M.K. Wu, *Proc. Natl. Acad. Sci. U.S.A.* **38**, 14262 (2008).
10. T.M. McQueen, Q. Huang, V. Ksenofontov, C. Felser, Q. Xu, H. Zandbergen, Y.S. Hor, J. Allred, A.J. Williams, D. Qu, J. Checkelsky, N.P. Ong, and R.J. Cava, *Phys. Rev.* **B79**, 014522 (2009).
11. E. Pomjakushina, K. Conder, V. Pomjakushin, M. Bendele, and R. Khasanov, *Phys. Rev.* **B80**, 024517 (2009).
12. K.-W. Yeh, T.-W. Huang, Y.-L. Huang, T.-K. Chen, F.-C. Hsu, P.M. Wu, Y.-C. Lee, Y.-Y. Chu, C.-L. Chen, J.-Y. Luo, D.C. Yan, and M.K. Wu, *Europhys. Lett.* **84**, 37002 (2008).
13. B.C. Sales, A.S. Sefat, M.A. McGuire, R. Jin, D. Mandrus, and Y. Mozharivskij, *Phys. Rev.* **B79**, 094521 (2009).
14. Y. Mizuguchi, F. Tomioka, S. Tsuda, T. Yamaguchi, and Y. Takano, *Appl. Phys. Lett.* **93**, 152505 (2008).
15. G. Garbarino, A. Sow, P. Lejay, A. Sulpice, P. Toulemonde, M. Mezouar, and M. Nunez-Regueiro, *Europhys. Lett.* **86**, 27001 (2009).
16. D. Braithwaite, B. Salce, G. Lapertot, F. Bourdarot, C. Marin, D. Aoki, and M. Hanfland, *J. Phys.: Condens. Matter* **21**, 232202 (2009).
17. S. Medvedev, T.M. McQueen, I.A. Troyan, T. Palasyuk, M.I. Erements, R.J. Cava, S. Naghavi, F. Casper, V. Ksenofontov, G. Wortmann, and C. Felser, *Nature Materials* **8**, 630 (2009).
18. S. Margadonna, Y. Takabayashi, Y. Ohishi, Y. Mizuguchi, Y. Takano, T. Kagayama, T. Nakagawa, M. Takata, and K. Prassides, *Phys. Rev.* **B80**, 064506 (2009).
19. A. Subedi, L. Zhang, D.J. Singh, and M.-H. Du, *Phys. Rev.* **B78**, 134514 (2008).
20. L. Zhang, D.J. Singh, and M.-H. Du, *Phys. Rev.* **B79**, 012506 (2009).
21. W. Bao, Y. Qiu, Q. Huang, M.A. Green, P. Zajdel, M.R. Fitzsimmons, M. Zhernenkov, M.H. Fang, B. Qian, E.K. Vehstedt, J.H. Yang, H.M. Pham, L. Spinu, and Z.Q. Mao, *Phys. Rev. Lett.* **102**, 247001 (2009).
22. S. Li, C. de la Cruz, Q. Huang, Y. Chen, J.W. Lynn, J. Hu, Y.-L. Huang, F.-C. Hsu, K.-W. Yeh, M.-K. Wu, and P. Dai, *Phys. Rev.* **B79**, 054503 (2009).
23. F. Ma, W. Ji, J. Hu, Z.-Y. Lu, and T. Xiang, *Phys. Rev. Lett.* **102**, 177003 (2009).
24. V. Tsurkan, J. Deisenhofer, A. G $\ddot{u}$ nter, Ch. Kant, H.-A. Krug von Nidda, F. Schrettle, and A. Loidl, *arXiv:1006.4453 v1* (2010).
25. M.H. Fang, H.M. Pham, B. Qian, T.J. Liu, E.K. Vehstedt, Y. Liu, L. Spinu, and Z.Q. Mao, *Phys. Rev.* **B78**, 224503 (2008).
26. F. Walz, *J. Phys.: Condens. Matter* **14**, R285 (2002).
27. J. Yang, M. Mansui, M. Kawa, H. Ohta, C. Michioka, C. Dong, H. Wang, H. Yuan, M. Fang, and K. Yoshimura, *J. Phys. Soc. Jpn.* **79**, 074704 (2010).
28. R. Viennois, E. Giannini, D. van der Marel, and R. Černý, *J. Solid State Chem.* (2010), *in press*.
29. R. Hu, E.S. Bozin, J.B. Warren, and C. Petrovic, *Phys. Rev.* **B80**, 214514 (2009).
30. S. Iikubo, M. Fujita, S. Niitaka, and H. Takagi, *J. Phys. Soc. Jpn.* **78**, 103704 (2009).
31. K.-W. Lee, V. Pardo, and W.E. Pickett, *Phys. Rev.* **B78**, 174502 (2008).
32. M.-J. Han and S.Y. Savrasov, *Phys. Rev. Lett.* **103**, 067001 (2009).
33. Y. Ding, Y. Wang, and J. Ni, *Solid State Commun.* **149**, 505 (2009).
34. S. Chadov, D. Scharf, G.H. Fecher, C. Felser, L. Zhang, and D.J. Singh, *Phys. Rev.* **B81**, 104523 (2010).
35. J.M. Wills, O. Eriksson, M. Alouani, and D.L. Price, in: *Electronic Structure and Physical Properties of Solids: the Uses of the LMTO Method*, H. Dreyse (ed.), Springer Verlag, Berlin (2000), p. 148; M. Alouani and J.M. Wills, *ibid.*, p. 168; O. Eriksson and J.M. Wills, *ibid.* p. 247.
36. G.E. Grechnev, R. Ahuja, and O. Eriksson, *Phys. Rev.* **B68**, 64414 (2003).
37. U. von Barth and L. Hedin, *J. Phys. C: Solid State Phys.* **5**, 1629 (1972).
38. L. Nordström, O. Eriksson, M.S.S. Brooks, and B. Johansson, *Phys. Rev.* **B41**, 9111 (1990).
39. A.V. Ruban, S. Khmelevskiy, P. Mohn, and B. Johansson, *Phys. Rev.* **B75**, 054402 (2007).